Science
AAAS

Observations of Biologically Generated Turbulence in a Coastal Inlet
Eric Kunze, *et al.*
Science **313**, 1768 (2006);
DOI: 10.1126/science.1129378

Science (print ISSN 0036-8075; online ISSN 1095-9203) is published weekly, except the last week in December, by the American Association for the Advancement of Science, 1200 New York Avenue NW, Washington, DC 20005.

zontal surfaces of the Homalite plates that were blocked by the hydraulic press) to the velocity measurement position. Also, the free surfaces (across the smallest dimension of the Homalite plates) did not act as barriers. We conjecture that the pulse formation was due either to the velocity-weakening character of the friction law or to the changes in the frictional resistance caused by non-uniform variations in dynamic normal stress on the rupture interface, or to a combination of both phenomena.

When the impact speed was further reduced to 10 m/s, the rupture mode became purely pulse-like (Fig. 3). The rupture started at A_1 and propagated at a sub-Rayleigh speed of 0.76 C_S, whereas, after 15 μs, the sliding ceased at A_2. The duration of sliding was very short compared to the ~100-μs duration of the impact event. Thus, we infer that an isolated pulse was formed. Such a case clearly indicates that a purely pulse-like mode of rupture can occur under the appropriate conditions.

References and Notes

1. J. R. Rice, in *Proceedings of the 20th International Congress of Theoretical and Applied Mechanics, 2000, Chicago*, H. Aref, J. W. Philips, Eds. (Kluwer Academic, Dordrecht, Netherlands, 2001), pp. 1–23.
2. A. J. Rosakis, *Adv. Phys.* **51**, 1189 (2002).
3. R. Madariaga, *Bull. Seismol. Soc. Am.* **66**, 639 (1976).
4. S. Das, K. Aki, *Geophys. J. Royal Astron. Soc.* **50**, 643 (1977).
5. S. M. Day, *Bull. Seismol. Soc. Am.* **72**, 705 (1982).
6. D. J. Andrews, *Bull. Seismol. Soc. Am.* **75**, 1 (1985).
7. R. A. Harris, S. M. Day, *J. Geophys. Res.* **98**, 4461 (1993).
8. T. H. Heaton, *Phys. Earth Planet. Inter.* **64**, 1 (1990).
9. S. H. Hartzell, T. H. Heaton, *Bull. Seismol. Soc. Am.* **73**, 1553 (1983).
10. H. L. Liu, D. V. Helmberger, *Bull. Seismol. Soc. Am.* **73**, 201 (1983).
11. S. Nielsen, R. Madariaga, *Bull. Seismol. Soc. Am.* **93**, 2375 (2003).
12. J. N. Brune, in *Seismic Risk and Engineering Decisions*, C. Lomnitz, E. Rosenbluth, Eds. (Elsevier, New York, 1976), pp. 141–171.
13. G. Di Toro, D. L. Goldsby, T. E. Tullis, *Nature* **427**, 436 (2004).
14. A. Cochard, R. Madariaga, *J. Geophys. Res.* **101**, 25,321 (1996).
15. N. M. Beeler, T. E. Tullis, *Bull. Seismol. Soc. Am.* **86**, 1130 (1996).
16. G. Perrin, J. R. Rice, G. Zheng, *J. Mech. Phys. Solids* **43**, 1461 (1995).
17. N. Lapusta, J. R. Rice, Y. Ben-Zion, G. Zheng, *J. Geophys. Res.* **105**, 23,765 (2000).
18. S. B. Nielsen, J. M. Carlson, K. B. Olsen, *J. Geophys. Res.* **105**, 6069 (2000).
19. D. Coker, G. Lykotrafitis, A. Needleman, A. J. Rosakis, *J. Mech. Phys. Solids* **53**, 884 (2005).
20. A. Cochard, J. Rice, *J. Geophys. Res.* **105**, 25891 (2000).
21. J. R. Rice, N. Lapusta, K. Ranjith, *J. Mech. Phys. Solids* **49**, 1865 (2001).
22. G. Zheng, J. R. Rice, *Bull. Seismol. Soc. Am.* **88**, 1466 (1998).
23. K. Aki, *J. Geophys. Res.* **84**, 140 (1979).
24. E. Johnson, *Geophys. J. Int.* **101**, 125 (1990).
25. E. Richardson, C. Marone, *J. Geophys. Res.* **104**, 28,859 (1999).
26. P. Bodin, S. Brown, D. Matheson, *J. Geophys. Res.* **103**, 29,931 (1998).
27. G. Lykotrafitis, A. J. Rosakis, G. Ravichandran, *Exper. Mech.* **46**, 205 (2006).
28. O. Samudrala, Y. Huang, A. J. Rosakis, *J. Geophys. Res.* **107**, 10129/2001JB000460 (2002).
29. A. Needleman, *J. Appl. Mech.* **66**, 847 (1999).
30. A. J. Rosakis, O. Samudrala, D. Coker, *Science* **284**, 1337 (1999).

31. The authors acknowledge the support of NSF (grant EAR 0207873) and the U.S. Department of Energy (grant DE-FG52-06NA26209). The consistent support of the Office of Naval Research through grant N00014-03-1-0435 (Y. D. S. Rajapakse, Program Manager) is also gratefully acknowledged. The authors also thank H. Kanamori, A. Needleman, D. Coker, and N. Lapusta for their many constructive suggestions.

Supporting Online Material

www.sciencemag.org/cgi/content/full/313/5794/1765/DC1
Materials and Methods
Figs. S1 to S5
Reference

5 April 2006; accepted 26 July 2006
10.1126/science.1128359

Observations of Biologically Generated Turbulence in a Coastal Inlet

Eric Kunze,[1]* John F. Dower,[1]* Ian Beveridge,[2] Richard Dewey,[1] Kevin P. Bartlett[1]

Measurements in a coastal inlet revealed turbulence that was three to four orders of magnitude larger during the dusk ascent of a dense acoustic-scattering layer of krill than during the day, elevating daily-averaged mixing in the inlet by a factor of 100. Because vertically migrating layers of swimming organisms are found in much of the ocean, biologically generated turbulence may affect (i) the transport of inorganic nutrients to the often nutrient-depleted surface layer from underlying nutrient-rich stratified waters to affect biological productivity and (ii) the exchange of atmospheric gases such as CO_2 with the stratified ocean interior, which has no direct communication with the atmosphere.

Turbulent mixing in the ocean plays key roles in a wide range of processes, from regulating the large-scale thermohaline overturning circulation (also known as the global conveyor belt) and water-mass modification, to the dispersal and dilution of anthropogenic waste. Below the surface mixed layer, turbulent mixing controls the exchange of water properties between the surface layer, which is in direct contact with the atmosphere, and the density-stratified ocean interior, where mixing is typically reduced to diffusivities on the order of 0.1×10^{-4} m^2 s^{-1} (*1*, *2*), controlled by the breaking of internal waves generated by the wind and tides. Exchange across the highly stratified base of the surface mixed layer influences not only biological productivity through nutrient supply but also air/sea gas exchange (*3*). By providing another mechanism by which nutrients and tracers can pass between the nutrient-limited surface mixed layer and the underlying nutrient-replete stratified ocean, biologically generated turbulence could (i) explain how surface production is often higher than can be accounted for by known mixing mechanisms (*4*) and (ii) regulate gas exchange between the ocean and atmosphere, which plays a key role in the carbon cycle, carbon sequestration, and climate.

Although marine organisms have long been known to be capable of generating turbulence (*5*–*8*), the role of biologically generated turbulent mixing in the ocean has largely been neglected, perhaps because this mechanism was discounted in earlier work (*9*). However, more recent evaluations based on the energetics of swimming organisms suggest that species ranging in size from large zooplankton (0.5 cm) to cetaceans on the order of 10 m long can generate turbulent dissipation rates ε (the rate at which turbulent kinetic energy is damped by molecular viscosity) on the order of 10^{-5} W kg^{-1} within schools and swarms (*10*, *11*). Such high values, fully three to four orders of magnitude larger than average turbulence levels in the stratified ocean, have the potential to dominate mixing in the upper ocean, where marine organisms are most abundant. Here we report observations quantifying biologically generated turbulence in a coastal inlet.

The above notion was tested by collecting microstructure profiles with depth during dusk in Saanich Inlet, British Columbia. The profiler measures microscale (1 cm) shear, temperature, and conductivity, as well as fine-scale (1 m) temperature, conductivity, and pressure. Profiles were collected at 3-min intervals. Microscale shear measurements were de-spiked before processing to remove plankton collisions. Following common practice, dissipation rates were estimated by iteratively fitting shear spectra from 4-m half-overlapping profile segments to a turbulence model spectrum (*12*). The wavenumber band from 1 to 100 cpm (wavelengths of 0.01 to 1 m) was typically fit for dissipation rates exceeding 10^{-7} W kg^{-1}. A shipboard 200-kHz ASL Environmental Sciences Water Column Profiler single-beam echosounder (*13*)

[1]School of Earth and Ocean Sciences, University of Victoria, Post Office Box 3055, STN CSC Victoria, BC, V8W-3P6, Canada. [2]Department of Biology, University of Victoria, Post Office Box 3020, STN CSC Victoria, BC, V8W-3N5, Canada.

*To whom correspondence should be addressed. E-mail: kunze@uvic.ca (E.K.); dower@uvic.ca (J.F.D.)

tracked the vertical movement of a dense acoustic-scattering layer of euphausiids. The echosounder transmitted 300-μs pulses at 1 Hz. Volume backscatter intensity was recorded in 0.125-m depth bins.

Saanich Inlet is a semi-enclosed fjord with a maximum depth of about 240 m. It is connected to the Strait of Georgia through narrow tidal channels with a 70-m sill. Typical turbulent dissipation rates in the inlet are less than 10^{-9} W kg^{-1} (*14*). Waters below about 100 m depth are anoxic because of bacterial decomposition of settled biomass. Despite weak winds and tides, the inlet is very productive in the summer. The supply of nutrients for this productivity is thought to arise from tidal mixing outside the inlet, followed by advection into the inlet by tidally rectified mean currents. This hypothesis is supported by a 14-day cycle in nutrients and blooms (*14*).

Saanich Inlet hosts a large resident population of the euphausiid (krill) *Euphausia pacifica*, which occur in concentrations of up to 10,000 individuals m^{-3}; that is, one krill every 5 cm (*15*, *16*). *E. pacifica* is the most common euphausiid in the coastal waters of the northeast Pacific and is an important prey item for many fish species, including herring (*17*). It is also a strong vertical migrator. During daylight, euphausiids in Saanich Inlet remain largely sedentary, resting just above the anoxic interface at about 100 m, presumably to hide from visual predators (*18*). As dusk approaches, the euphausiids swim toward the surface, with the smallest individuals preceding the largest 2-cm-long individuals by approximately 20 min (*19*). Laboratory studies have shown that, at peak swimming speeds, individual *E. pacifica* generate a jet with maximum speeds of about 5 cm s^{-1} (*20*). Acoustic observations of the *E. pacifica* population in Saanich Inlet suggest average ascent speeds of 2.5 to 3.5 cm s^{-1} (*21*). At dawn, the largest individuals begin the descent, followed by smaller individuals. This size bias in the timing of ascent and descent has been interpreted as further evidence of predator avoidance; smaller animals ascend earlier and descend later because they are less visible to predators than are larger animals (*22*, *23*).

Our measurements took place during late April 2005. Winds were very light throughout. Waters below 5 m depth were strongly stratified, with buoyancy frequencies of 10^{-2} rad s^{-1}. Even higher stratifications were found above, with well-mixed surface layer thicknesses not exceeding 3 m. During daylight, the dense backscattering layer of krill remained stationary at about 100 m, and turbulent dissipation rates ε were close to the instrument noise level of 10^{-9} W kg^{-1} (Fig. 1), which is comparable to signals typically found in the open ocean (*1*). At dusk on 28 April, the backscattering layer began to ascend and become more diffuse. Initially, no enhanced microstructure was observed. However, as the base of the scattering layer [thought to be associated with larger euphausiids, with Reynolds numbers sufficiently high to generate turbulence (*10*)] began to shoal, turbulence levels between 30 and 100 m depth approached 10^{-5} to 10^{-4} W kg^{-1} for a 10- to 15-min interval. These values are 100 to 1000 times the dissipation rates associated with turbulence patches in the stratified deep ocean and are comparable to values found in strongly turbulent tidal channels (*1*, *24*). Corresponding diffusivities during this interval were 200 × 10^{-4} m^2 s^{-1} to 2000 × 10^{-4} m^2 s^{-1}. Density remained well stratified during the measurement interval, so turbulence cannot be attributed to mixed-layer deepening; during the sampling interval, 3-m temperature decreased by 3°C because of surface cooling or horizontal advection, but this surface-intensified cooling was confined to a depth of 15 m or less. The microstructure shear spectra produced resemble those associated with shear-driven turbulence, and unstable density overturns of 1 to 10 m during this interval are consistent with the above dissipation rates. This is at odds with the 1.5-cm length of individual krill, suggesting that they act in concert rather than as individuals when they swim upward. By acting communally, they would reduce viscous drag.

The backscattering layer ascended 100 m in less than 15 min, which is consistent with the swimming speeds recorded in the lab of 5 to 10 cm s^{-1} (*20*). Because the period of peak ascent lasted less than 15 min, it is not difficult to imagine how it could have been undersampled

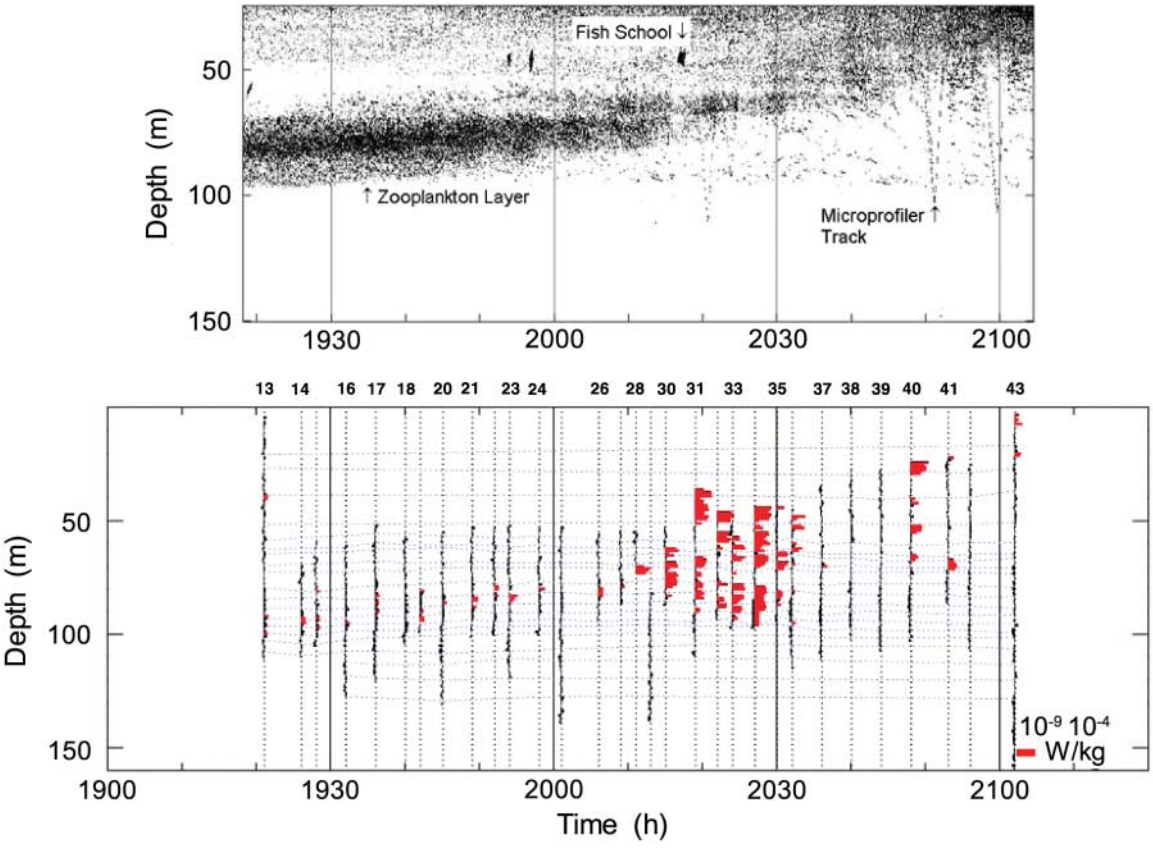

Fig. 1. Profile time series in Saanich Inlet spanning about 100 min during dusk on 28 April 2005. (**Top**) Acoustic backscatter data from a 200-kHz echosounder reveals vertical migration of the backscatter layer. The lowering and raising of the vertical microstructure profiler is also evident for some profiles. (**Bottom**) Turbulent dissipation rate log(ε) (red, index lower right) with vertical dotted lines denoting profile times and horizontal dotted lines denoting salinity or density surfaces. For profiles 13 to 29, dissipation rates are on the order of 10^{-9} W kg^{-1}. For profiles 30 to 36, spanning 17 min, dissipation rates are two to four orders of magnitude higher before falling back to background levels of about 10^{-9} W kg^{-1} for the remainder of the time series.

by previous microstructure measurements. Despite its short duration, this episode was sufficient to boost daily-averaged turbulent eddy diffusivities in Saanich Inlet by two to three orders of magnitude. Daily-averaged diffusivities are 0.02×10^{-4} m^2 s^{-1} when dusk and dawn enhancement are excluded but 4×10^{-4} m^2 s^{-1} to 40×10^{-4} m^2 s^{-1} when they are included.

On a second day of sampling, the sky was overcast. At dusk, the backscattering layer began to migrate, though slightly later than the previous evening. Unlike the first evening, no discernible enhancement of turbulence was observed in the microstructure data. The acoustic data suggest that, for reasons unknown, the lower portion of the backscattering layer (the part most likely composed of the largest euphausiids) remained at depth. We hypothesize that larger euphausiids did not migrate, so that little or no turbulence was generated on the second night.

Several key groups of marine organisms, ranging from krill, to small pelagics such as herring and anchovies, to tuna, occur in sufficient abundance and in sufficiently dense schools to contribute substantial turbulent mixing, particularly in coastal waters (*10*). Our results confirm this for euphausiids in Saanich Inlet. The measured dissipation rates on the order of 10^{-5} W kg^{-1} are consistent with levels predicted for the Antarctic krill *E. superba* (*10*).

These data raise the possibility that a potentially important source of mixing in biologically productive parts of the upper ocean has been overlooked. Further data collected during June 2006 confirm the major results (*25*). Because many densely schooling species, particularly strong vertical migrators, are active near the base of the mixed layer, episodic biologically enhanced turbulence deserves further attention.

References and Notes

1. M. C. Gregg, *J. Geophys. Res.* **92**, 5249 (1987).
2. J. R. Ledwell, A. J. Watson, C. S. Law, *Nature* **364**, 701 (1993).
3. R. C. Hamme, S. R. Emerson, *J. Mar. Res.* **64**, 73 (2006).
4. W. Jenkins, S. Doney, *Global Biogeochem. Cycles* **17**, article no. 1110 (2003).
5. S. Vogel, *Life in Moving Fluids: The Physical Biology of Flow* (Princeton Univ. Press, Princeton, NJ, 1981).
6. U. Müller, B. van den Heuvel, E. Stamhuis, J. Videler, *J. Exp. Biol.* **200**, 2893 (1997).
7. J. Y. Cheng, G. Chahine, *Comp. Biochem. Physiol. A* **131**, 51 (2001).
8. J. Videler, E. Stamhuis, U. Müller, L. van Duren, *Integr. Comp. Biol.* **45**, 988 (2002).
9. W. Munk, *Deep-Sea Res.* **13**, 707 (1966).
10. M. E. Huntley, M. Zhou, *Mar. Ecol. Prog. Ser.* **273**, 65 (2004).
11. W. K. Dewar *et al.*, *J. Mar. Res.* **64**, 541 (2006).
12. R. K. Dewey, W. R. Crawford, *J. Phys. Oceanogr.* **18**, 1161 (1988).
13. A. S. Brierley *et al.*, *Limno. Oceanogr. Methods* **4**, 18 (2006).
14. A. E. Gargett, D. Stucchi, F. Whitney, *Estuar. Coast. Shelf Sci.* **56**, 1141 (2003).
15. C. F. Greenlaw, *Limnol. Oceanogr.* **24**, 226 (1979).
16. G. O. Mackie, C. E. Mills, *Can. J. Fish. Aquat. Sci.* **40**, 763 (1983).
17. M. Mangel, S. Nicol, *Can. J. Fish. Aquat. Sci.* **57** (suppl. 3), 1 (2000).
18. J. S. Jaffe, M. D. Ohman, A. De Robertis, *Can. J. Fish. Aquat. Sci.* **56**, 2000 (1999).
19. A. De Robertis, J. S. Jaffe, M. D. Ohman, *Limnol. Oceanogr.* **45**, 1838 (2000).
20. J. Yen, J. Brown, D. R. Webster, *Mar. Fresh. Behav. Physiol.* **36**, 307 (2003).
21. A. De Robertis, C. Schell, J. S. Jaffe, *J. Mar. Sci.* **60**, 885 (2003).
22. O. Yamamura, I. Inada, K. Shimazaki, *Mar. Biol.* **132**, 195 (1998).
23. A. De Robertis, *Limnol. Oceanogr.* **47**, 925 (2002).
24. A. E. Gargett, *J. Atmos. Oceanic Tech* **16**, 1973 (1999).
25. Measurements spanning three dusks and two dawns during 10 to 12 June 2006 found no discernible enhancement at the first dusk after an overcast day. After the sunny second and third days, elevated dissipation rates associated with vertical migration of the acoustic backscattering layer were observed during both dusk and dawn.
26. Data were collected with help from K. Brown and the crew of the *R/V Strickland*. Valuable comments were provided by J. Nash, T. Miller, J. MacKinnon, L. St. Laurent, W. Dewar, B. Legget, and R. Campbell. This research was made possible by the British Columbia Knowledge Development Foundation, the Canada Foundation for Innovation, the National Sciences and Engineering Council of Canada, and funds available to E.K. under the Canada Research Chair program.

1 May 2006; accepted 26 July 2006
10.1126/science.1129378

Solid Ammonium Sulfate Aerosols as Ice Nuclei: A Pathway for Cirrus Cloud Formation

J. P. D. Abbatt,[1]* S. Benz,[2] D. J. Cziczo,[3] Z. Kanji,[1] U. Lohmann,[3] O. Möhler[2]

Laboratory measurements support a cirrus cloud formation pathway involving heterogeneous ice nucleation by solid ammonium sulfate aerosols. Ice formation occurs at low ice-saturation ratios consistent with the formation of continental cirrus and an interhemispheric asymmetry observed for cloud onset. In a climate model, this mechanism provides a widespread source of ice nuclei and leads to fewer but larger ice crystals as compared with a homogeneous freezing scenario. This reduces both the cloud albedo and the longwave heating by cirrus. With the global ammonia budget dominated by agricultural practices, this pathway might further couple anthropogenic activity to the climate system.

Accurate representation of cirrus clouds remains a challenge to climate modeling, in part because of an incomplete understanding of ice cloud formation mechanisms (*1*). Whereas ice formation studies have been performed at higher temperatures (*2*), only recently has the cold cirrus regime been addressed. This has led to a homogeneous freezing model where ice nucleates directly from the aerosol aqueous phase (*3*). Heterogeneous freezing occurs through selective nucleation onto a small fraction of the background particles (*2*) at lower ice-saturation ratios (S_{ice}) than with homogeneous freezing. Traditionally, it has been thought that good heterogeneous ice nuclei are insoluble solids, such as mineral dust (*2*). Recently, it has been shown in the laboratory that soluble species can also act as ice nuclei in both the immersion (*4*, *5*) and deposition modes (*6*). In the latter case, Shilling *et al.* (*6*) demonstrated that roughly 1 in 10^5 supramicrometer-sized particles of solid ammonium sulfate on a cold plate act as ice nuclei at low ice supersaturations, suggesting that this could be an important atmospheric process. Here, we report measurements of the onset for deposition ice formation on solid ammonium sulfate aerosol under experimental conditions similar to those in the cirrus regime, and we assess the impact of this new ice formation mechanism on past laboratory experiments, field observations, and global climate.

Measurements at Storm Peak, CO, implicate a role of ammoniated particles in selective ice nucleation at low S_{ice} (*7*). It was observed that between 10^{-4} and 10^{-5} of the particles were heterogeneous ice nuclei. Of this fraction, roughly 25% were not classified as conventional insoluble ice nuclei particles—i.e., they did not contain substantial levels of mineral dust, elemental carbon, metal, or fly ash. Instead, these ice nuclei were sulfates, with some degree of organics present. Although the degree of neutralization of the particles was not measured, continental sulfate aerosol likely contains a large amount of ammonium (*8*).

These observations of selective heterogeneous ice nucleation on continental sulfate particles are consistent with laboratory ice nucleation experiments. Figure 1 presents data for two aerosol types representative of sulfate aerosol endpoints. H_2SO_4 particles exist in remote settings away from

[1]Department of Chemistry, University of Toronto, Toronto, ON M5S 3H6, Canada. [2]Institute for Meteorology and Climate Research (IMK-AAF), Forschungszentrum Karlsruhe, Postfach 3640, 76021 Karlsruhe, Germany. [3]Institute for Atmospheric and Climate Science, ETH Zurich, 8092, Zurich, Switzerland.

*To whom correspondence should be addressed. E-mail: jabbatt@chem.utoronto.ca